Statistical Properties of Wideband MIMO Mobile-to-Mobile Channels

Alenka G. Zajić and Gordon L. Stüber
School of Electrical and Computer Engineering
Georgia Institute of Technology, Atlanta, GA 30332 USA

***Abstract*— A three-dimensional (3-D) theoretical model for wideband multiple-input multiple-output (MIMO) mobile-to-mobile (M-to-M) channels is presented. Based on this model, the statistical properties of wideband MIMO M-to-M channels are derived. In particular, the space-time-frequency correlation function, the power space-delay spectral density, and the envelope level crossing rate are derived for a 3-D non-isotropic scattering environment. Finally, to validate the theoretical derivations, some simulation results are presented and compared with measured data.**

I. Introduction

Mobile-to-mobile (M-to-M) communications play an important role in mobile ad-hoc wireless networks, intelligent transportation systems, and relay-based cellular networks. M-to-M communication systems are equipped with low elevation antennas and have both the transmitter ($\mathrm{T_x}$) and the receiver ($\mathrm{R_x}$) in motion. To successfully design M-to-M systems, it is necessary to have a detailed knowledge of the outdoor multipath fading channel and its statistical properties. The statistical properties of M-to-M channels are quite different from conventional fixed-to-mobile (F-to-M) cellular land mobile radio channels [1]. Akki and Haber [2] proposed a reference model for single-input single-output (SISO) M-to-M Rayleigh fading channels. The reference models for narrowband multiple-input multiple-output (MIMO) M-to-M channels have been proposed in [3], [4]. The previously reported models are two-dimensional (2-D) and accurate only for certain environments, e.g., rural areas. For urban environments where the $\mathrm{T_x}$ and $\mathrm{R_x}$ antenna arrays are often located in close proximity to and lower than surrounding buildings, the tree-dimensional (3-D) models are more appropriate. Hence, we have recently proposed the three-dimensional (3-D) reference models for *narrowband* and *wideband* MIMO M-to-M multipath fading channels [5], [6] as well as the simulation models for wideband MIMO M-to-M channels [7].

This paper uses the 3-D reference model in [6] to derive the statistical properties of wideband MIMO M-to-M channels. The 3-D reference model generates the input delay-spread function as a superposition of the line-of-sight (LoS), single-bounced and double-bounced rays. The parametric nature of the model makes it adaptable to a variety of propagation environments, i.e., outdoor micro- and macro-cells. Based on this model, the space-time-frequency correlation function (stf-cf), the power space-delay spectral density (psds), and the envelope level crossing rate (LCR) are derived for a 3-D non-isotropic scattering environment. Finally, to verify the theoretical derivations, some simulation results are presented and compared with measured data in [8], and [9].

The remainder of the paper is organized as follows. Section II presents the geometrical "concentric-cylinders" model and the 3-D parametric reference model for wideband MIMO M-to-M channels. Section III derives the stf-cf, the psds, and the LCR for a 3-D non-isotropic scattering environment. Section IV presents some simulation results to verify theoretical derivations. Finally, Section V provides some concluding remarks.

II. A 3-D Theoretical Model for Wideband MIMO Mobile-to-Mobile Channels

This section describes a 3-D theoretical model for wideband MIMO M-to-M multipath fading channels. We consider a MIMO communication system with L_t transmit and L_r receive omnidirectional antenna elements. It is assumed that both the $\mathrm{T_x}$ and $\mathrm{R_x}$ are in motion and equipped with low elevation antennas. The radio propagation in outdoor micro- and macro-cells is characterized by 3-D wide sense stationary uncorrelated scattering (WSSUS) with either line-of-sight (LoS) or non-line-of-sight (NLoS) conditions between the $\mathrm{T_x}$ and $\mathrm{R_x}$. The MIMO channel is described by an $L_r \times L_t$ matrix $\mathbf{H}(t,\tau) = [h_{ij}(t,\tau)]_{L_r \times L_t}$ of the input delay-spread functions.

Fig. 1 shows the 3-D "concentric-cylinders" geometrical model with $L_t = L_r = 2$ antenna elements. The "concentric-cylinders" model defines four cylinders, two around the $\mathrm{T_x}$ and another two around the $\mathrm{R_x}$, as shown in Fig. 1. Around the $\mathrm{T_x}$, M fixed omnidirectional scatterers occupy a volume between cylinders of radii R_{t1} and R_{t2}. It is assumed that the M scatterers lie on L cylindric surfaces of radii $R_{t1} \leq R_t^{(l)} \leq R_{t2}$, where $1 \leq l \leq L$. The l^{th} cylindric surface contains $M^{(l)}$ fixed omnidirectional scatterers, and the $(m,l)^{th}$ transmit scatterer is denoted by $S_T^{(m,l)}$. Similarly, around the $\mathrm{R_x}$, N fixed omnidirectional scatterers occupy a volume between cylinders of radii R_{r1} and R_{r2}. It is assumed that N scatterers lie on K cylindric surfaces of radii $R_{r1} \leq R_r^{(k)} \leq R_{r2}$, where $1 \leq k \leq K$. The k^{th} cylindric surface contains $N^{(k)}$ fixed omnidirectional scatterers, and the $(n,k)^{th}$ receive scatterer is

0 Prepared through collaborative participation in the Collaborative Technology Alliance for Communications & Networks sponsored by the U.S. Army Research Laboratory under Cooperative Agreement DAAD19-01-2-0011. The U.S. Government is authorized to reproduce and distribute reprints for Government purposes notwithstanding any copyright notation thereon.

denoted by $S_R^{(n,k)}$. The parameters in Fig. 1 are defined in Table I.

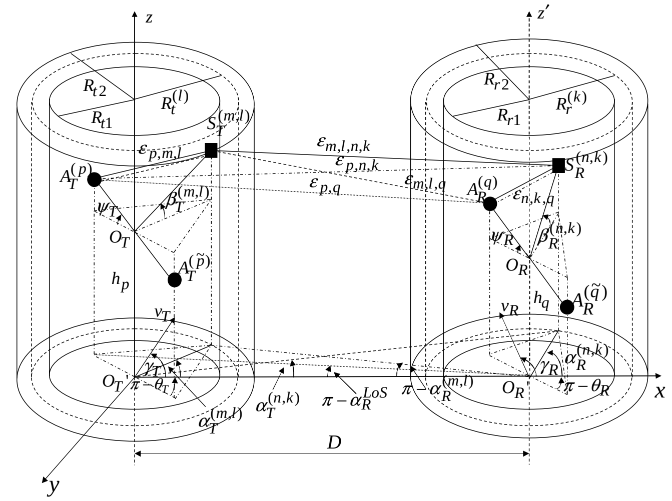

Fig. 1. The "concentric-cylinders" model with LoS, single- and double-bounced rays for a MIMO M-to-M channel with $L_t = L_r = 2$ antenna elements.

It is assumed that the radii R_{t2} and R_{r2} are much smaller than the distance D, i.e., $\max\{R_{t2}, R_{r2}\} \ll D$ (local scattering condition for outdoor micro- and macro-cells). Furthermore, it is assumed that the distance D is smaller than $4R_{t1}R_{r1}L_r/(\lambda(L_t-1)(L_r-1))$ (channel does not experience keyhole behavior [10]), where λ denotes the carrier wavelength. Finally, it is assumed that d_T and d_R are much smaller than the radii R_{t1} and R_{r1}, i.e., $\max\{d_T, d_R\} \ll \min\{R_{t1}, R_{r1}\}$.

From the 3-D geometrical model, we observe that waves from the $\mathrm{T_x}$ antenna elements traverse directly to the $\mathrm{R_x}$ antenna elements or they are single- or double-bounced before arriving at the $\mathrm{R_x}$ antenna elements. Hence, the input delay-spread function of the link $A_T^{(p)}$ - $A_R^{(q)}$ can be written as a superposition of the LoS, single-bounced, and double-bounced rays [6], i.e., $h_{pq}(t,\tau)$ is equal to

$$h_{pq}^{SBT}(t,\tau) + h_{pq}^{SBR}(t,\tau) + h_{pq}^{DB}(t,\tau) + h_{pq}^{LoS}(t,\tau). \quad (1)$$

To simplify further derivations, we will use the time-variant transfer function (i.e., the Fourier transformation of the input delay-spread function), which can be written as

$$\begin{aligned} T_{pq}(t,f) &= \mathcal{F}_\tau\{h_{pq}(t,\tau)\} = T_{pq}^{SBT}(t,f) + T_{pq}^{SBR}(t,f) \\ &+ T_{pq}^{DB}(t,f) + T_{pq}^{LoS}(t,f). \end{aligned} \quad (2)$$

The single- and double-bounced components of the time-variant transfer function are, respectively,

$$T_{pq}^{SBT}(t,f) = \sqrt{\eta_T} \lim_{M\to\infty} \sum_{l=1}^{L} \sum_{m=1}^{M^{(l)}} \xi_{m,l} g_{m,l}(t) e^{-j2\pi f \tau_{m,l}}, (3)$$

$$T_{pq}^{SBR}(t,f) = \sqrt{\eta_R} \lim_{N\to\infty} \sum_{k=1}^{K} \sum_{n=1}^{N^{(k)}} \xi_{n,k} g_{n,k}(t) e^{-j2\pi f \tau_{n,k}}, \quad (4)$$

$$T_{pq}^{DB}(t,f) = \quad (5)$$
$$\sqrt{\eta_{TR}} \lim_{M,N\to\infty} \sum_{l,m=1}^{L,M^{(l)}} \sum_{k,n=1}^{K,N^{(k)}} \xi_{m,l,n,k} g_{m,l,n,k}(t) e^{-j2\pi f \tau_{m,l,n,k}},$$

where parameters $\xi_{m,l}$, $\xi_{n,k}$, $\xi_{m,l,n,k}$, $\tau_{m,l}$, $\tau_{n,k}$, and $\tau_{m,l,n,k}$

TABLE I

DEFINITION OF PARAMETERS IN FIGURE 1.

D	The distance between the centers of the Tx and Rx cylinders.
$R_t^{(l)}$, $R_r^{(k)}$	The radius of the l^{th} Tx and k^{th} Rx cylinder, respectively.
d_T , d_R	The spacing between antenna elements at the Tx and Rx, respectively.
θ_T , θ_R	The orientation of the Tx and Rx antenna array in the x-y plane (relative to the *x*-axis), respectively.
ψ_T , ψ_R	The elevation of the Tx's and Rx's antenna array relative to the x-y plane, respectively.
v_T , v_R	The velocities of the Tx and Rx, respectively.
γ_T , γ_R	The moving directions of the Tx and Rx, respectively.
$\alpha_T^{(m,l)}$, $\alpha_T^{(n,k)}$	The azimuth angles of departure (AAoD) of the waves that impinge on the scatterers $S_T^{(m,l)}$ and $S_R^{(n,k)}$, respectively.
$\alpha_R^{(m,l)}$, $\alpha_R^{(n,k)}$	The azimuth angles of arrival (AAoA) of the waves scattered from $S_T^{(m,l)}$ and $S_R^{(n,k)}$, respectively.
α_R^{LoS}	The AAoA of the LoS paths.
$\beta_T^{(m,l)}$, $\beta_R^{(n,k)}$	The elevation angles of departure (EAoD) and the elevation angles of arrival (EAoA), respectively.
$\varepsilon_{p,m,l}$, $\varepsilon_{m,l,q}$, $\varepsilon_{p,n,k}$, $\varepsilon_{n,k,q}$, $\varepsilon_{m,l,n,k}$ and ε_{pq}	The distances $d\left(A_T^{(p)}, S_T^{(m,l)}\right)$, $d\left(S_T^{(m,l)}, A_R^{(q)}\right)$, $d\left(A_T^{(p)}, S_R^{(n,k)}\right)$, $d\left(S_T^{(m)}, S_R^{(n)}\right)$, $d\left(S_R^{(n,k)}, A_R^{(q)}\right)$, $d\left(S_T^{(m,l)}, S_R^{(n,k)}\right)$, and $d\left(A_T^{(p)}, A_R^{(q)}\right)$, respectively
h_T , h_R	The distances $d\left(O_T, O_T^{'}\right)$ and $d\left(O_R, O_R^{'}\right)$, respectively.

denote amplitudes of the multipath components and time delays, respectively. Functions $g_{m,l}(t)$, $g_{n,k}(t)$, and $g_{m,l,n,k}(t)$ are defined as follows

$$g_{m(n),l(k)}(t) = e^{-j\frac{2\pi}{\lambda}\left(\epsilon_{p,m/n,l/k}+\epsilon_{m/n,l/k,q}\right)+j\phi_{m/n,l/k}} \quad (6)$$
$$\times\ e^{j2\pi t\left[f_{T\max}\cos\ \alpha_T^{(m/n,l/k)}-\gamma_T\ +f_{R\max}\cos\ \alpha_R^{(m/n,l/k)}-\gamma_R\ \right]},$$
$$g_{m,l,n,k}(t) = e^{-j\frac{2\pi}{\lambda}(\epsilon_{p,m,l}+\epsilon_{m,l,n,k}+\epsilon_{n,k,q})+j\phi_{m,l,n,k}} \quad (7)$$
$$\times\ e^{j2\pi t\left[f_{T\max}\cos\ \alpha_T^{(m,l)}-\gamma_T\ +f_{R\max}\cos\ \alpha_R^{(n,k)}-\gamma_R\ \right]},$$

where $f_{T\max} = v_T/\lambda$ and $f_{R\max} = v_R/\lambda$ are the maximum Doppler frequencies associated with the $\mathrm{T_x}$ and $\mathrm{R_x}$, respectively, and λ is the carrier wavelength. The amplitudes $\xi_{m,l}$, $\xi_{n,k}$, and $\xi_{m,l,n,k}$ are approximated as

$$\xi_{m,l} \approx \frac{\Omega_{pq}\left(1-\frac{\gamma}{2}\frac{R_t^{(l)}}{D}\right)}{\sqrt{M(K_{pq}+1)}}, \quad (8)$$

$$\xi_{n,k} \approx \frac{\Omega_{pq}\left(1-\frac{\gamma}{2}\frac{R_r^{(k)}}{D}\right)}{\sqrt{N(K_{pq}+1)}}, \quad (9)$$

$$\xi_{m,l,n,k} \approx \frac{\Omega_{pq}}{\sqrt{MN(K_{pq}+1)}}\left(1-\frac{\gamma}{2}\frac{R_t^{(l)}+R_r^{(k)}}{2D}\right), \quad (10)$$

where $\Omega_{pq} = D^{-\gamma/2}\sqrt{P_{pq}}\lambda/4\pi$, P_{pq} is the power transmitted through the subchannel $A_T^{(p)}$ - $A_R^{(q)}$, K_{pq} denotes the Rice factor (ratio of LoS to scatter received power) of the subchannel $A_T^{(p)}$ - $A_R^{(q)}$, and γ is the path loss exponent. The time delays $\tau_{m,l}$ and $\tau_{m,l,n,k}$ are defined as the travel times of the waves scattered from the scatterers $S_T^{(m,l)}$ and $S_R^{(n,k)}$, i.e. $\tau_{m,l} = D/c_0 + R_t^{(l)}(1 - \cos\alpha_T^{(m,l)})/c_0 \cos\beta_T^{(m,l)}$ and $\tau_{n,k} = D/c_0 + R_r^{(k)}(1+\cos\alpha_R^{(n,k)})/c_0\cos\beta_R^{(n,k)}$, respectively, where c_0 is the speed of light. Finally, the time delay $\tau_{m,l,n,k}$ is defined as the travel time of the wave impinged on the scatterer $S_T^{(m,l)}$ and scattered from the scatterer $S_R^{(n,k)}$, i.e. $\tau_{m,l,n,k} = D/c_0 + R_t^{(l)}(1-\cos\alpha_T^{(m,l)})/c_0\cos\beta_T^{(m,l)} + R_r^{(k)}(1+\cos\alpha_R^{(n,k)})/c_0\cos\beta_R^{(n,k)}$. Parameters η_T, η_R, and η_{TR} specify how much the single- and double-bounced rays contribute in the total power P_{pq}, i.e., these parameters satisfy $\eta_T + \eta_R + \eta_{TR} = 1$. It is assumed that the angles of departure ($\alpha_T^{(m,l)}$ and $\beta_T^{(m,l)}$), the angles of arrival ($\alpha_R^{(n,k)}$ and $\beta_R^{(n,k)}$), and the radii $R_t^{(l)}$ and $R_r^{(k)}$ are random variables, and that the angles of departure and radii $R_t^{(l)}$ are independent from the angles of arrival and radii $R_r^{(k)}$. Note that the AAoA, $\alpha_R^{(m,l)}$, is a function of the AAoD, $\alpha_T^{(m,l)}$, and the AAoD, $\alpha_T^{(n,k)}$, is a function of the AAoA, $\alpha_R^{(n,k)}$ and, hence, they are not independent angular variables. Additionally, it is assumed that the phases $\phi_{m,l}$, $\phi_{n,k}$, and $\phi_{m,l,n,k}$ are random variables uniformly distributed on the interval $[-\pi,\pi)$ and independent from the angles of departure, the angles of arrival, and the radii of the cylinders. The LoS component of the time-variant transfer function is

$$T_{pq}^{LoS}(t,f) = \sqrt{\frac{K_{pq}}{K_{pq}+1}}\xi_{LoS}g_{LoS}(t)e^{-j2\pi f\tau_{LoS}}, \quad (11)$$

where $\xi_{LoS} \approx \Omega_{pq}$, $\tau_{LoS} = \sqrt{D^2+\Delta H^2}/c_0$, $g^{LoS}(t) = e^{j2\pi t[f_{R\max}\cos(\alpha_R^{LoS}-\gamma_R)+f_{T\max}\cos(\pi-\alpha_R^{LoS}-\gamma_T)]-j\frac{2\pi}{\lambda}\epsilon_{p,q}}$, and $\Delta H = (h_p - h_q)/2$. Finally, the distances $\epsilon_{m,l,q}$, $\epsilon_{p,n,k}$, $\epsilon_{p,m,l}$, $\epsilon_{n,k,q}$, $\epsilon_{p,q}$, and $\epsilon_{m,l,n,k}$ can be expressed as functions of the random variables $\alpha_T^{(m,l)}$, $\beta_T^{(m,l)}$, $\alpha_R^{(n,k)}$, $\beta_R^{(n,k)}$, α_{Rq}^{LoS}, $R_t^{(l)}$, and $R_r^{(k)}$ as follows:

$$\begin{aligned}
\epsilon_{m,l,q} &\approx D - (0.5L_r + 0.5 - q)(d_{Ry}\Delta_T^{(l)}\sin\alpha_T^{(m,l)} - d_{Rx}),\\
\epsilon_{p,n,k} &\approx D - (0.5L_t + 0.5 - p)(d_{Ty}\Delta_R^{(k)}\sin\alpha_R^{(n,k)} + d_{Tx}),\\
\epsilon_{p,m,l} &\approx R_t^{(l)} - (0.5L_t + 0.5 - p)\big[d_{Tz}\sin\beta_T^{(m,l)} +\\
&\quad d_{Tx}\cos\alpha_T^{(m,l)}\cos\beta_T^{(m,l)} + d_{Ty}\sin\alpha_T^{(m,l)}\cos\beta_T^{(m,l)}\big],\\
\epsilon_{n,k,q} &\approx R_r^{(k)} - (0.5L_r + 0.5 - q)\big[d_{Rz}\sin\beta_R^{(n,k)} +\\
&\quad d_{Rx}\cos\alpha_R^{(n,k)}\cos\beta_R^{(n,k)} + d_{Ry}\sin\alpha_R^{(n,k)}\cos\beta_R^{(n,k)}\big],\\
\epsilon_{p,q} &\approx D - (0.5L_t + 0.5 - p)d_{Tx} -\\
&\quad (0.5L_r + 0.5 - q)d_R\cos\psi_R\cos(\alpha_{Rq}^{LoS} - \theta_R),\\
\epsilon_{m,l,n,k} &\approx D, \qquad (12)
\end{aligned}$$

where parameters p and q take values from the sets $p \in \{1,\ldots,L_t\}$ and $q \in \{1,\ldots,L_r\}$, $d_{Tx} = d_T\cos\psi_T\cos\theta_T$, $d_{Ty} = d_T\cos\psi_T\sin\theta_T$, $d_{Rx} = d_R\cos\psi_R\cos\theta_R$, $d_{Ry} = d_R\cos\psi_R\sin\theta_R$, $d_{Tz} = d_T\sin\psi_T$, $d_{Rz} = d_R\sin\psi_R$, $\Delta_T^{(l)} = R_t^{(l)}/D$, and $\Delta_R^{(k)} = R_r^{(k)}/D$. Derivations of the expressions in (12) are omitted for brevity.

III. Statistical Properties of Wideband MIMO M-to-M Channels

This section derives the stf-cf, the psds, and the LCR for a 3-D non-isotropic scattering environment. The normalized stf-cf between two time-variant transfer functions $T_{pq}(t,f)$ and $T_{\tilde{p}\tilde{q}}(t,f)$ is defined as

$$R_{pq,\tilde{p}\tilde{q}}(\Delta t,\Delta f) = \frac{\mathrm{E}\left[T_{pq}(t,f)^* T_{\tilde{p}\tilde{q}}(t+\Delta t, f+\Delta f)\right]}{\sqrt{\mathrm{E}[|T_{pq}(t,f)|^2]\mathrm{E}[|T_{\tilde{p}\tilde{q}}(t,f)|^2]}}, \quad (13)$$

where $(\ \cdot\ )^*$ denotes complex conjugate operation, $\mathrm{E}[\ \cdot\ ]$ is the statistical expectation operator, $p,\tilde{p} \in \{1,\ldots,L_t\}$, and $q,\tilde{q} \in \{1,\ldots,L_r\}$. Since the number of local scatterers in the reference model is infinite, the discrete AAoDs, $\alpha_T^{(m,l)}$, EAoDs, $\beta_T^{(m,l)}$, AAoAs, $\alpha_R^{(n,k)}$, EAoAs, $\beta_R^{(n,k)}$, and radii $R_t^{(l)}$ and $R_r^{(k)}$ can be replaced with continuous random variables α_T, β_T, α_R, β_R, R_t, and R_r. To characterize the random azimuth angles α_T and α_R, we use the von Mises probability density function (pdf) defined as [11] $f(\theta) = \exp[k\cos(\theta-\mu)]/2\pi I_0(k)$, where $\theta \in [-\pi,\pi)$, $I_0(\ \cdot\ )$ is the zeroth-order modified Bessel function of the first kind, $\mu \in [-\pi,\pi)$ is the mean angle at which the scatterers are distributed in the x - y plane, and k controls the spread of scatterers around the mean. To characterize the random elevation angles β_T and β_R, we use the pdf [12] $f(\varphi) = \pi\cos(\pi\varphi/(4\varphi_m))/(4|\varphi_m|)$ for $|\ \varphi\ | \le |\ \varphi_m\ | \le \pi/2$ and $f(\varphi) = 0$ otherwise. The parameter φ_m is the maximum elevation angle and lies in the range $0° \le |\ \varphi_m\ | \le 20°$ [13], [6]. To characterize the radii R_t and R_r, we use the pdfs [6] $f(R_t) = 2R_t/(R_{t2}^2 - R_{t1}^2)$ and $f(R_r) = 2R_r/(R_{r2}^2 - R_{r1}^2)$, respectively. Using trigonometric transformations, the equality $\int_{-\pi}^{\pi}\exp\{a\sin(c)+b\cos(c)\}dc = 2\pi I_0\left(\sqrt{a^2+b^2}\right)$ [14, eq. 3.338-4], and the results in [5], the stf-cfs of the single- and double-bounced components can be written as

$$R_{pq,\tilde{p}\tilde{q}}^{SBT}(d_T,d_R,\Delta t,\Delta f) \approx \quad (14)$$
$$\frac{\eta_T}{I_0(k_T)}\frac{\cos\left(\frac{2\pi}{\lambda}\beta_{Tm}d_{Tz}\right)}{1-\left(\frac{4\beta_{Tm}d_{Tz}}{\lambda}\right)^2}e^{-j\frac{2\pi}{\lambda}(q-\tilde{q})d_{Rx}}e^{-j2\pi\Delta t f_{R\max}\cos\gamma_R}$$
$$\int_{R_{t1}}^{R_{t2}} I_0\left(\sqrt{x_{SBT}^2 + y_{SBT}^2}\right)\frac{2R_t\left(1-\gamma\frac{R_t}{D}\right)e^{-j\frac{2\pi}{c_0}\Delta f(D+R_t)}}{R_{t2}^2 - R_{t1}^2}dR_t,$$
$$R_{pq,\tilde{p}\tilde{q}}^{SBR}(d_T,d_R,\Delta t,\Delta f) \approx \quad (15)$$
$$\frac{\eta_R}{I_0(k_R)}\frac{\cos\left(\frac{2\pi}{\lambda}\beta_{Rm}d_{Rz}\right)}{1-\left(\frac{4\beta_{Rm}d_{Rz}}{\lambda}\right)^2}e^{j\frac{2\pi}{\lambda}(p-\tilde{p})d_{Tx}}e^{j2\pi\Delta t f_{T\max}\cos\gamma_T}$$
$$\int_{R_{r1}}^{R_{r2}} I_0\left(\sqrt{x_{SBR}^2 + y_{SBR}^2}\right)\frac{2R_r\left(1-\gamma\frac{R_r}{D}\right)e^{-j\frac{2\pi}{c_0}\Delta f(D+R_r)}}{R_{r2}^2 - R_{r1}^2}dR_r,$$
$$R_{pq,\tilde{p}\tilde{q}}^{DB}(d_T,d_R,\Delta t,\Delta f) \approx \quad (16)$$
$$A_{DB}\int_{R_{t1}}^{R_{t2}} e^{-j\frac{2\pi}{c_0}\Delta f R_t}R_t I_0\left(\sqrt{x_{DB}^2 + y_{DB}^2}\right)dR_t$$
$$\times \int_{R_{r1}}^{R_{r2}} e^{-j\frac{2\pi}{c_0}\Delta f R_r}R_r I_0\left(\sqrt{w_{DB}^2 + z_{DB}^2}\right)\left(1-\gamma\frac{R_r}{D}\right)dR_r +$$

$$A_{DB}\int_{R_{r1}}^{R_{r2}} e^{-j\frac{2\pi}{c_0}\Delta f R_r} R_r I_0\left(\sqrt{w_{DB}^2+z_{DB}^2}\right) dR_r$$
$$\times \int_{R_{t1}}^{R_{t2}} e^{-j\frac{2\pi}{c_0}\Delta f R_t} R_t I_0\left(\sqrt{x_{DB}^2+y_{DB}^2}\right)\left(1-\gamma\frac{R_t}{D}\right) dR_t,$$

where $x_{SBT} \approx j2\pi[(p-\tilde{p})d_{Tx}/\lambda + \Delta t f_{T\max}\cos\gamma_T + \Delta f R_t/c_0] + k_T\cos\mu_T$, $y_{SBT} \approx j2\pi[(p-\tilde{p})d_{Ty}/\lambda + (q-\tilde{q})d_{Ry}\Delta_T/\lambda + \Delta t f_{T\max}\sin\gamma_T + \Delta t f_{R\max}\Delta_T\sin\gamma_R] + k_T\sin\mu_T$, $x_{SBR} \approx j2\pi[(q-\tilde{q})d_{Rx}/\lambda + \Delta t f_{R\max}\cos\gamma_R - \Delta f R_r/c_0] + k_R\cos\mu_R$, $y_{SBR} \approx j2\pi[(q-\tilde{q})d_{Ry}/\lambda + (p-\tilde{p})d_{Ty}\Delta_R/\lambda + \Delta t f_{R\max}\sin\gamma_R + \Delta t f_{T\max}\Delta_R\sin\gamma_T] + k_R\sin\mu_R$, $x_{DB} \approx j2\pi[(p-\tilde{p})d_{Tx}/\lambda + \Delta t f_{T\max}\cos\gamma_T + \Delta f R_t/c_0] + k_T\cos\mu_T$, $y_{DB} \approx j2\pi[(p-\tilde{p})d_{Ty}/\lambda + \Delta t f_{T\max}\sin\gamma_T] + k_T\sin\mu_T$, $z_{DB} \approx j2\pi[(q-\tilde{q})d_{Rx}/\lambda + \Delta t f_{R\max}\cos\gamma_R - \Delta f R_r/c_0] + k_R\cos\mu_R$, $w_{DB} \approx j2\pi[(q-\tilde{q})d_{Ry}/\lambda + \Delta t f_{R\max}\sin\gamma_R] + k_R\sin\mu_R$, and $A_{DB} = \eta_{TR}\cos(2\pi\beta_{Tm}d_{Tz}/\lambda)\cos(2\pi\beta_{Rm}d_{Rz}/\lambda)2e^{-j2\pi\Delta f D/c_0} / I_0(k_T)I_0(k_R)(1-(4\beta_{Tm}d_{Tz}/\lambda)^2)(1-(4\beta_{Rm}d_{Rz}/\lambda)^2)(R_{t2}^2 - R_{t1}^2)(R_{r2}^2 - R_{r1}^2)$. The integrals in (14) - (16) must be evaluated numerically, because they do not have closed-form solutions. Using (11) and approximation $\alpha_{Rq}^{LoS} = \alpha_{R\tilde{q}}^{LoS} \approx \pi$, the stf-cf of the LoS component can be approximated as

$$R_{pq,\tilde{p}\tilde{q}}^{LoS}(d_T, d_R, \Delta t, \Delta f) \approx \sqrt{K_{pq}K_{\tilde{p}\tilde{q}}} e^{j\frac{2\pi}{\lambda}[(p-\tilde{p})d_{Tx} - (q-\tilde{q})d_{Rx}]} e^{j2\pi\Delta t[f_{T\max}\cos\gamma_T - f_{R\max}\cos\gamma_R] - \frac{2\pi}{c_0}\Delta f\sqrt{D^2+\Delta H^2}}. \quad (17)$$

Finally, the normalized stf-cf between two time-variant transfer functions $T_{pq}(t,f)$ and $T_{\tilde{p}\tilde{q}}(t,f)$ becomes a summation of the stf-cfs in (14) - (17).

The psds of the time-variant transfer function is the inverse Fourier transformation of the space-frequency correlation function $R_{pq,\tilde{p}\tilde{q}}(d_T, d_R, \Delta t = 0, \Delta f)$. Using the equality [14, eq. 6.677-3] and after extensive calculations, the psds of the single- and double-bounced components become

$$P_{pq,\tilde{p}\tilde{q}}^{SBT}(d_T, d_R, \tau_{\text{rel}}) = \frac{\eta_T}{I_0(k_T)} \frac{\cos\left(\frac{2\pi}{\lambda}\beta_{T_m}d_{Tz}\right)}{1-\left(\frac{4\beta_{T_m}d_{Tz}}{\lambda}\right)^2} e^{-j\frac{2\pi}{\lambda}(q-\tilde{q})d_{Rx}}$$
$$\times \frac{2}{R_{t2}^2 - R_{t1}^2}\int_{R_{ta}}^{R_{tb}}\left(1-\gamma\frac{R_t}{D}\right) R_t e^{j\frac{2\pi}{c_0}R_t B_{SBT}(c_0\tau_{\text{rel}}/R_t - 1)}$$
$$\times \frac{\cosh\left(2jC_{SBT}\sqrt{\frac{c_0\tau_{\text{rel}}}{2R_t}\left(1-\frac{c_0\tau_{\text{rel}}}{2R_t}\right)}\right)}{\frac{2\pi}{c_0}R_t\sqrt{\frac{c_0\tau_{\text{rel}}}{2R_t}\left(1-\frac{c_0\tau_{\text{rel}}}{2R_t}\right)}} dR_t, \quad (18)$$

$$P_{pq,\tilde{p}\tilde{q}}^{SBR}(d_T, d_R, \tau_{\text{rel}}) = \frac{\eta_R}{I_0(k_R)} \frac{\cos\left(\frac{2\pi}{\lambda}\beta_{R_m}d_{Rz}\right)}{1-\left(\frac{4\beta_{R_m}d_{Rz}}{\lambda}\right)^2} e^{j\frac{2\pi}{\lambda}(p-\tilde{p})d_{Tx}}$$
$$\times \frac{2}{R_{r2}^2 - R_{r1}^2}\int_{R_{ra}}^{R_{rb}}\left(1-\gamma\frac{R_r}{D}\right) R_r e^{j\frac{2\pi}{c_0}R_r B_{SBR}(c_0\tau_{\text{rel}}/R_r - 1)}$$
$$\times \frac{\cosh\left(2jC_{SBR}\sqrt{\frac{c_0\tau_{\text{rel}}}{2R_r}\left(1-\frac{c_0\tau_{\text{rel}}}{2R_r}\right)}\right)}{\frac{2\pi}{c_0}R_r\sqrt{\frac{c_0\tau_{\text{rel}}}{2R_r}\left(1-\frac{c_0\tau_{\text{rel}}}{2R_r}\right)}} dR_r, \quad (19)$$

$$P_{pq,\tilde{p}\tilde{q}}^{DB}(d_T, d_R, \tau_{\text{rel}}) = \frac{\eta_{TR}}{I_0(k_T)I_0(k_R)} \frac{\cos\left(\frac{2\pi}{\lambda}\beta_{T_m}d_{Tz}\right)}{1-\left(\frac{4\beta_{T_m}d_{Tz}}{\lambda}\right)^2}$$
$$\times \frac{\cos\left(\frac{2\pi}{\lambda}\beta_{R_m}d_{Rz}\right)}{1-\left(\frac{4\beta_{R_m}d_{Rz}}{\lambda}\right)^2} \frac{2}{(R_{r2}^2 - R_{r1}^2)(R_{t2}^2 - R_{t1}^2)}\left[\int_{R_{ta}}^{R_{tb}} R_t\ F_t\right.$$
$$\times \frac{\cosh\left(2jC_{DB}\sqrt{\frac{c_0\tau_{\text{rel}}}{2R_t}\left(1-\frac{c_0\tau_{\text{rel}}}{2R_t}\right)}\right)}{\frac{2\pi}{c_0}R_t\sqrt{\frac{c_0\tau_{\text{rel}}}{2R_t}\left(1-\frac{c_0\tau_{\text{rel}}}{2R_t}\right)}} dR_t \odot \int_{R_{ra}}^{R_{rb}} R_r\ F_r$$
$$\times \left(1-\gamma\frac{R_r}{D}\right)\frac{\cosh\left(2jE_{DB}\sqrt{\frac{c_0\tau_{\text{rel}}}{2R_r}\left(1-\frac{c_0\tau_{\text{rel}}}{2R_r}\right)}\right)}{\frac{2\pi}{c_0}R_r\sqrt{\frac{c_0\tau_{\text{rel}}}{2R_r}\left(1-\frac{c_0\tau_{\text{rel}}}{2R_r}\right)}} dR_r +$$
$$\int_{R_{ta}}^{R_{tb}} R_t F_t\left(1-\gamma\frac{R_t}{D}\right)\frac{\cosh\left(2jC_{DB}\sqrt{\frac{c_0\tau_{\text{rel}}}{2R_t}\left(1-\frac{c_0\tau_{\text{rel}}}{2R_t}\right)}\right)}{\frac{2\pi}{c_0}R_t\sqrt{\frac{c_0\tau_{\text{rel}}}{2R_t}\left(1-\frac{c_0\tau_{\text{rel}}}{2R_t}\right)}} dR_t$$
$$\left.\odot \int_{R_{ra}}^{R_{rb}} R_r\ F_r \frac{\cosh\left(2jE_{DB}\sqrt{\frac{c_0\tau_{\text{rel}}}{2R_r}\left(1-\frac{c_0\tau_{\text{rel}}}{2R_r}\right)}\right)}{\frac{2\pi}{c_0}R_r\sqrt{\frac{c_0\tau_{\text{rel}}}{2R_r}\left(1-\frac{c_0\tau_{\text{rel}}}{2R_r}\right)}} dR_r\right], \quad (20)$$

where $\cosh(\ \cdot\ )$ is the hyperbolic cosine, $\odot$ denotes convolution, $\tau_{\text{rel}} = \tau - D/c_0$, $F_t = e^{j2\pi R_t B_{DB}(c_0\tau_{\text{rel}}/R_t - 1)/c_0}$, $F_r = e^{j2\pi R_r D_{DB}(c_0\tau_{\text{rel}}/R_r - 1)/c_0}$ $B_{DB} = ((p-\tilde{p})d_{Tx}/\lambda - jk_T\cos\mu_T)/\pi\tau_t$, $C_{DB} = (p-\tilde{p})d_{Ty}/\lambda - jk_T\sin\mu_T$, $\tau_t = 2R_t/c_0$, $D_{DB} = ((q-\tilde{q})d_{Rx}/\lambda - jk_R\cos\mu_R)/\pi\tau_r$, $E_{DB} = (q-\tilde{q})d_{Ry}/\lambda - jk_R\sin\mu_R$, and $\tau_r = 2R_r/c_0$. The integrals in (18) - (20) need to be numerically evaluated over all possible radii R_t and R_r, respectively. For the range $0 \le \tau_{\text{rel}} \le 2R_{t1}/c_0$, integration limits are $R_{ta} = R_{t1}$, $R_{tb} = R_{t2}$, $R_{ra} = R_{r1}$, and $R_{rb} = R_{r2}$. On the other hand, when $2R_{t1}/c_0 \le \tau_{\text{rel}} \le 2R_{t2}/c_0$, integration limits are $R_{ta} = c_0\tau_{\text{rel}}/2$, $R_{tb} = R_{t2}$, $R_{ra} = c_0\tau_{\text{rel}}/2$, and $R_{rb} = R_{r2}$. The psds of the LoS component is obtained by calculating the inverse Fourier transformation of the space-frequency correlation function in (17) and can be written as

$$P_{pq,\tilde{p}\tilde{q}}^{LoS}(d_T, d_R, \tau_{\text{rel}}) = \sqrt{K_{pq}K_{\tilde{p}\tilde{q}}} e^{j\frac{2\pi}{\lambda}[(p-\tilde{p})d_{Tx} - (q-\tilde{q})d_{Rx}]} \delta\left(\tau - \frac{\sqrt{D^2+\Delta H^2}}{c_0}\right), \quad (21)$$

where $\delta(\ \cdot\ )$ denotes the Dirac delta function. Finally, the psds $P_{pq,\tilde{p}\tilde{q}}(d_T, d_R, \tau_{\text{rel}})$ between two time-variant transfer functions $T_{pq}(t=0,f)$ and $T_{\tilde{p}\tilde{q}}(t=0,f)$ becomes a summation of the psds in equations (18) - (21).

The LCR at a specified level R, $L(R)$, is defined as the rate at which the signal envelope crosses level R in the positive (or negative) going direction. When a LoS component is present, the LCR can be calculated as [15]

$$L(R) = \frac{2R\sqrt{K+1}}{\pi^{3/2}}\sqrt{\frac{b_2}{b_0} - \frac{b_1^2}{b_0^2}}\ e^{-K-(K+1)R^2}$$

$$
\times \quad \int_0^{\pi/2} \cosh\Big(2\sqrt{K(K+1)}R\cos\theta\Big)
$$

$$
\times \quad \Big[e^{-(\chi\sin\theta)^2} + \sqrt{\pi}\chi\sin\theta \ \mathrm{erf}(\chi\sin\theta)\Big]\, d\theta, \quad (22)
$$

where $\cosh(\ \cdot\ )$ is the hyperbolic cosine function, $\mathrm{erf}(\ \cdot\ )$ is the error function, and the parameter χ is equal to $\sqrt{Kb_1^2/(b_0b_2-b_1^2)}$, and K denotes the averaged Rice factor. Finally, parameters b_0, b_1, and b_2 are defined as [16]

$$
b_0 \ \stackrel{\triangle}{=}\ \mathrm{E}[h_i(t,\tau=0)^2] = \mathrm{E}[h_q(t,\tau=0)^2], \quad (23)
$$

$$
b_1 \ \stackrel{\triangle}{=}\ \mathrm{E}[h_i(t,0)\dot{h}_q(t,0)] = \mathrm{E}[h_q(t,0)\dot{h}_i(t,0)], \quad (24)
$$

$$
b_2 \ \stackrel{\triangle}{=}\ \mathrm{E}[\dot{h}_i(t,0)^2] = \mathrm{E}[\dot{h}_q(t,0)^2], \quad (25)
$$

where $h_i(t,0)$ and $h_q(t,0)$ denote the in-phase and quadrature component of the input delay-spread function $h(t,0) = h^{SBT}(t,0) + h^{SBR}(t,0) + h^{DB}(t,0)$, $\mathrm{E}[\ \cdot\ ]$ denotes the statistical expectation operator, and $\dot{h}_i(t,0)$ and $\dot{h}_q(t,0)$ denote the first derivative of $h_i(t,0)$ and $h_q(t,0)$ with respect to time t. The parameters b_0, b_1, and b_2 are obtained by substituting (1) into (23), (24) and (25), respectively, and by using trigonometric transformations, and the equality $\int_{-\pi}^{\pi} e^{-jm\theta+jz\sin\theta}d\theta = 2\pi J_m(z)$ [14, eq. 8.411], where $J_m(\ \cdot\ )$ is the m^{th}-order Bessel function of the first kind. After extensive calculations, the parameters b_0, b_1, and b_2 become

$$
b_n \quad = \quad b_n^{SBT} + b_n^{SBR} + b_n^{DB}, \quad (26)
$$

where $n \in \{0,1,2\}$, $b_0^{SBT(R)} = \eta_{T(R)}/(K+1)$, $b_0^{DB} = \eta_{TR}/(K+1)$, and the parameters $b_1^{SBT(R)}$, b_1^{DB}, $b_2^{SBT(R)}$, and b_2^{DB} are, respectively,

$$
b_1^{SBT(R)} = \frac{\eta_{T(R)}}{K+1}\Bigg\{\frac{\pi^2\cos\beta_{T(R)_m}}{\pi^2-4\beta_{T(R)_m}^2}2\pi f_{T(R)\max}\frac{I_1(k_{T(R)})}{I_0(k_{T(R)})}
$$

$$
\times\cos\big(\mu_{T(R)}-\gamma_{T(R)}\big) - \Bigg[2\pi f_{R(T)\max}\Delta_{T(R)}\sin\gamma_{R(T)}
$$

$$
\times\ \sin\mu_{T(R)}\frac{I_1(k_{T/R})}{I_0(k_{T/R})} \pm\ 2\pi f_{R(T)\max}\cos\gamma_{R(T)}\Bigg] \quad (27)
$$

$$
\times\frac{\pi^2[\cos(\Delta_{T(R)}\beta_{T(R)_m}+\frac{\Delta_H}{D})+\cos(\Delta_{T(R)}\beta_{T(R)_m}-\frac{\Delta_H}{D})]}{2[\pi^2-4\Delta_{T(R)}^2\beta_{T(R)_m}^2]}\Bigg\},
$$

$$
b_1^{DB} = \frac{\eta_{TR}}{K+1}\Bigg\{\frac{\pi^2\cos\beta_{T_m}}{\pi^2-4\beta_{T_m}^2}2\pi f_{T\max}\cos(\mu_T-\gamma_T)\frac{I_1(k_T)}{I_0(k_T)}
$$

$$
+\frac{\pi^2\cos\beta_{R_m}}{\pi^2-4\beta_{R_m}^2}2\pi f_{R\max}\cos(\mu_R-\gamma_R)\frac{I_1(k_R)}{I_0(k_R)}\Bigg\}, \quad (28)
$$

$$
b_2^{SBT(R)} = \frac{(2\pi)^2\eta_{T(R)}}{K+1}\Bigg\{f_{T(R)\max}^2\Bigg[\frac{\pi^2\cos(2\beta_{T(R)_m})}{2(\pi^2-16\beta_{T(R)_m}^2)}+\frac{1}{2}\Bigg]
$$

$$
\times\frac{1+\cos(2(\mu_{T(R)}-\gamma_{T(R)}))I_2(k_{T(R)})}{2I_0(k_{T(R)})} + \quad (29)
$$

$$
\Bigg[\cos((\Delta_{T(R)}-1)\beta_{T(R)_m}+\frac{\Delta_H}{D})+\cos((\Delta_{T(R)}+1)\beta_{T(R)_m}+\frac{\Delta_H}{D})
$$

$$
+\cos((\Delta_{T(R)}-1)\beta_{T(R)_m}-\frac{\Delta_H}{D})+\cos((\Delta_{T(R)}+1)\beta_{T(R)_m}-\frac{\Delta_H}{D})\Bigg]
$$

$$
\frac{4\beta_{T(R)_m}^2+8\Delta_{T(R)}\beta_{T(R)_m}^2-\pi^2+4\Delta_{T(R)}^2\beta_{T(R)_m}^2}{4\beta_{T(R)_m}^4[\frac{8\pi^2}{\beta_{T(R)_m}^2}-16-\frac{\pi^4}{\beta_{T(R)_m}^4}-16\Delta_{T(R)}^4+\frac{8\Delta_{T(R)}^2}{\beta_{T(R)_m}^2}+32\Delta_{T(R)}^2]}
$$

$$
\times\Bigg[f_{T(R)\max}f_{R(T)\max}\Delta_{T(R)}\sin\gamma_{R(T)}\Bigg(\cos\gamma_{T(R)}-\frac{I_2(k_{T(R)})}{I_0(k_{T(R)})}
$$

$$
\times\cos(2\mu_{T(R)}-\gamma_{T(R)})\Bigg)\mp 2f_{T(R)\max}f_{R(T)\max}\cos\gamma_{R(T)}\Bigg] +
$$

$$
\Bigg[\frac{\cos\left[2\left(\Delta_{T(R)}\beta_{T(R)_m}+\frac{\Delta_H}{D}\right)\right]\pi^2+2\pi^2-32\Delta_{T(R)}^2\beta_{T(R)_m}^2}{4[\pi^2-16\Delta_{T(R)}^2\beta_{T(R)_m}]}
$$

$$
+\frac{\cos\left[2\left(\Delta_{T(R)}\beta_{T(R)_m}-\frac{\Delta_H}{D}\right)\right]\pi^2}{4[\pi^2-16\Delta_{T(R)}^2\beta_{T(R)_m}]}\Bigg]\Bigg[f_{R(T)\max}^2\cos\gamma_{R(T)}^2
$$

$$
+f_{R(T)\max}^2\Delta_{T(R)}^2\sin\gamma_{R(T)}^2\frac{1-\cos(2\mu_{T(R)})I_2(k_{T(R)})}{2I_0(k_{T(R)})}
$$

$$
\pm f_{R(T)\max}^2\Delta_{T(R)}\sin(2\gamma_{R(T)})\sin\mu_{T(R)}\frac{I_1(k_{T(R)})}{I_0(k_{T(R)})}\Bigg]\Bigg\},
$$

$$
b_2^{DB} = \frac{(2\pi)^2\eta_{TR}}{K+1}\Bigg\{f_{T\max}^2\frac{\pi^2(\cos(2\beta_{T_m})+1)-16\beta_{T_m}^2}{2(\pi^2-16\beta_{T_m}^2)} \quad (30)
$$

$$
\times\frac{1+\cos(2(\mu_T-\gamma_T))I_2(k_T)}{2I_0(k_T)} + f_{T\max}f_{R\max}\frac{\pi^2\cos\beta_{T_m}}{\pi^2-4\beta_{T_m}^2}
$$

$$
\times\frac{2\pi^2\cos\beta_{R_m}}{\pi^2-4\beta_{R_m}^2}\cos(\mu_T-\gamma_T)\frac{I_1(k_T)}{I_0(k_T)}\cos(\mu_R-\gamma_R)\frac{I_1(k_R)}{I_0(k_R)}
$$

$$
+f_{R\max}^2\Bigg[\frac{\pi^2\cos(2\beta_{R_m})}{2(\pi^2-16\beta_{R_m}^2)}+\frac{1}{2}\Bigg]\frac{1+\cos(2(\mu_R-\gamma_R))I_2(k_R)}{2I_0(k_R)}\Bigg\}.
$$

IV. Simulation Results

In this section, we present some simulation results to verify theoretical derivations. In Figs. 2 and 3, we plot the psds, $P_{pq,\tilde{p}\tilde{q}}(d_T, d_R, \tau_{\mathrm{rel}})$, for several MIMO systems. In these

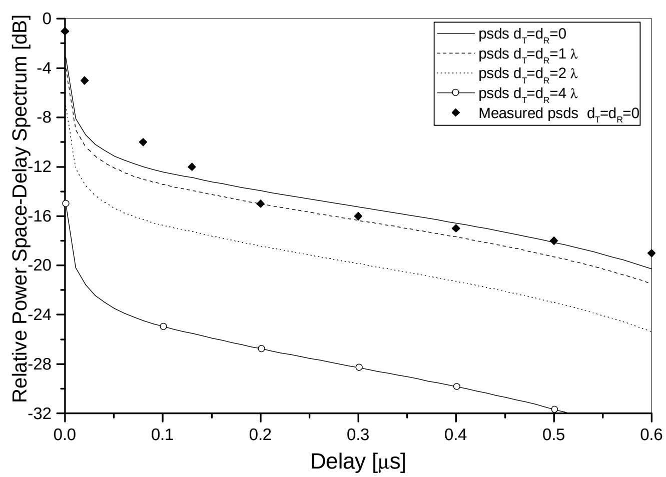

Fig. 2. The theoretical and measured relative power space-delay spectra characteristic for the outdoor M-to-M micro-cell propagation.

figures, we analyze the radio propagation in outdoor M-to-M micro- and macro-cells, assuming 3-D non-isotropic scattering ($k_T = k_R = 9.4$ for curves in Fig. 2 and $k_T = k_R = 9.1$ for curves in Fig. 3) and non-line-of-sight ($K = 0$) conditions between the transmitter and receiver. Parameters

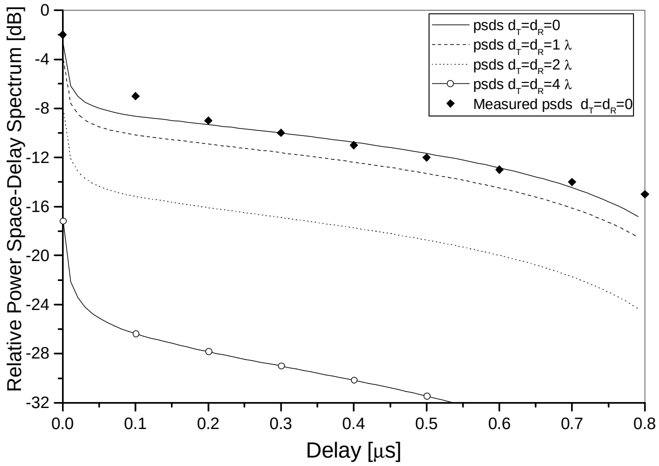

Fig. 3. The theoretical and measured relative power space-delay spectra characteristic for the outdoor M-to-M macro-cell propagation.

used to obtain curves in Figs. 2 and 3 are $\beta_{Tm} = \beta_{Rm} = 15°$, $\theta_T = \theta_R = \pi/4$, $\psi_T = \psi_R = \pi/3$, $\gamma_T = \gamma_R = 0$, $\mu_T = \pi/2$, $\mu_R = 3\pi/2$, $\lambda = 0.3$ m, $R_{t1} = R_{r1} = 20$ m, $R_{t2} = R_{r2} = 110$ m, $D = 5$ km, $\gamma = 4$, $L_t = L_r = 2$, and $d_T = d_R \in \{0, 1\ \lambda,\ 2\ \lambda,\ 4\ \lambda\}$. In Fig. 2, we assume that the single-bounced rays bear more energy ($\eta_T = \eta_R = 0.45$) than the double-bounced rays ($\eta_{TR} = 0.1$), which is characteristic for the outdoor M-to-M micro-cell propagation. We can observe that the M-to-M micro-cell psds has two distinct slopes and dies out after 0.6 μs. In Fig. 3, we consider the macro-cell propagation, i.e. $\eta_T = \eta_R = 0.2$ and $\eta_{TR} = 0.6$). In this case, the psds closely follows the one-sided exponential function dies out after 0.8 μs. Compared to measured relative power delay spectra for SISO system taken from Fig. 2 [8], our theoretical relative power space-delay spectra for $d_T = d_R = 0$ closely match. Finally, Fig. 4 compares the analytical LCR with the measured LCR taken from Fig. 8 of [9]. The measured data are collected on the highway in Germany [9]. The analytical LCR is obtained

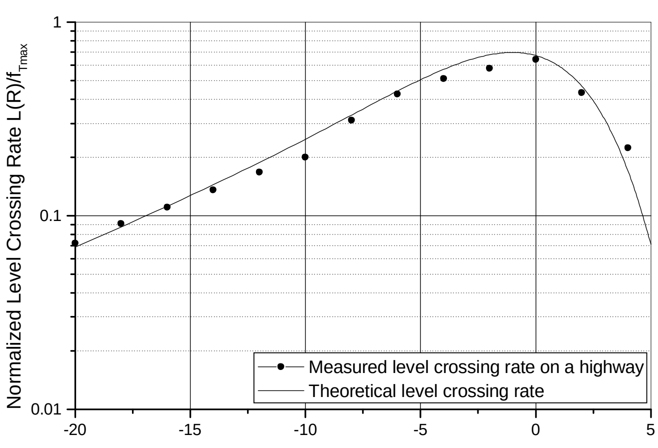

Fig. 4. The analytical and measured level crossing rate characteristic for a highway.

using the parameters $K = 1.73$, $\mu_T = 31.2°$, $k_T = 18.2$, $\beta_{T_m} = 10°$, $\Delta_T = \Delta_R = 0.6$, $\mu_R = 216.3°$, $k_R = 10.6$, $\beta_{R_m} = 5°$, $\eta_T = 0.36$, $\eta_R = 0.22$, $\eta_{TR} = 0.42$, $D = 300$ m, $\gamma_T = \gamma_R = \Delta_H = 0$, and $f_{T\max} = f_{R\max} = 500$ Hz. Fig. 4 shows the close agreement between the theoretical and empirical LCR.

The close agreement between the theoretical and empirical curves in Figs. 2 - 4 confirms the utility of the proposed wideband model.

V. Conclusions

This paper presented the 3-D theoretical model for wideband MIMO M-to-M channels. Based on this model, the stf-cf, the psds, and the LCR are derived for a 3-D non-isotropic scattering environment. Finally, some simulation results are presented and compared with measured data.

Disclaimer

The views and conclusions contained in this document are those of the authors and should not be interpreted as representing the official policies, either expressed or implied, of the Army Research Laboratory or the U. S. Government.

References

[1] A. S. Akki, "Statistical properties of mobile-to-mobile land communication channels," *IEEE Trans. on Veh. Tech.*, pp. 826–831, Nov. 1994.

[2] A.S. Akki and F. Haber, "A statistical model for mobile-to-mobile land communication channel," *IEEE Trans. Veh. Tech.*, pp. 2–10, Feb. 1986.

[3] M. Pätzold, B.O. Hogstad, N. Youssef, and D. Kim, "A MIMO mobile-to-mobile channel model: Part I-the reference model," *Proc. IEEE PIMRC'05*, vol. 1, pp. 573–578, Germany, Sept. 2005.

[4] A.G. Zajić and G.L. Stüber, "Space-Time Correlated MIMO Mobile-to-Mobile Channels," *Proc. IEEE PIMRC'06*, Finland, Sept. 2006.

[5] A.G. Zajić and G.L. Stüber, "A Three-Dimensional MIMO Mobile-to-Mobile Channel Model," *IEEE WCNC'07*, Hong Kong, Mar. 2007.

[6] A.G. Zajić and G.L. Stüber, "A three dimensional parametric model for wideband MIMO mobile-to-mobile channels," *Proc. IEEE GLOBECOM*, Washington, D.C., USA, Nov. 2007.

[7] A.G. Zajić and G.L. Stüber, "A 3-D simulation models for wideband MIMO mobile-to-mobile channels," *Proc. IEEE MILCOM*, Orlando, FL, USA, Oct. 2007.

[8] G. Acosta and M. A. Ingram, "Model development for the wideband expressway vehicle-to-vehicle 2.4 GHz channel," *Proc. IEEE WCNC'06*,vol. 3, pp. 1283–1288, Las Vegas, NE, USA, April 2006.

[9] J. Maurer, T. Fügen, and W. Wiesbeck, "Narrow-band measurement and analysis of the inter-vehicle transmission channel at 5.2 GHz,"*Proc. IEEE VTC*, pp. 1274–1278, Birmingham, AL, USA, May 2002.

[10] D. Gesbert, H. Bölcskei, D.A. Gore, and A.J. Paulraj, "Outdoor MIMO wireless channels: models and performance prediction," *IEEE Trans. on Commun.*, vol. 50, pp. 1926–1934, Dec. 2002.

[11] A. Abdi, J. A. Barger, and M. Kaveh, "A parametric model for the distribution of the angle of arrival and the associated correlation function and power spectrum at the mobile station," *IEEE Trans. on Veh. Tech.*, vol. 51, pp. 425–434, May 2002.

[12] J.D. Parsons and A.M.D. Turkmani, "Characterisation of mobile radio signals: model description," *IEE Proc. I, Commun., Speach, and Vision*, vol. 138, pp. 549–556, Dec. 1991.

[13] A. Kuchar, J.-P. Rossi, and E. Bonek, "Directional macro-cell channel characterization from urban measurements," *IEEE Trans. on Antennas and Propagation*, vol. 48, pp. 137–146, Feb. 2000.

[14] I.S. Gradshteyn and I.M. Ryzhik, *Table of Integrals, Series, and Products 5^{th} ed.*. A. Jeffrey, Ed. San Diego CA: Academic, 1994.

[15] M. Pätzold, U. Killat, and F. Laue, "An extended Suzuki model for land mobile satellite channels and its statistical properties,"*IEEE Trans. on Veh. Tech.*, vol. 47, pp. 617–630, May 1998.

[16] W. C. Jakes, *Microwave Mobile Communications*, 2nd ed. Piscataway, NJ: Wiley-IEEE Press, 1994.